Inorganic Chemistry

pubs.acs.org/IC

Review

Structural Chemistry of Zeolitic Imidazolate Frameworks

Zhiling Zheng,[⊥] Zichao Rong,[⊥] Ha L. Nguyen,[⊥] and Omar M. Yaghi*

Cite This: *Inorg. Chem.* 2023, 62, 20861−20873

Read Online

ACCESS | Metrics & More | Article Recommendations | Supporting Information

ABSTRACT: Zeolitic imidazolate frameworks (ZIFs) are a subclass of reticular structures based on tetrahedral four-connected networks of zeolites and minerals. They are composed of transition-metal ions and imidazolate-type linkers, and their pore size and shape, surface area, and functionality can be precisely controlled. Despite their potential, two questions remain unanswered: how to synthesize more diverse ZIF structures and how ZIFs differentiate from other crystalline solids. In other words, how can we use our understanding of their unique structures to better design and synthesize ZIFs? In this Review, we first summarize the methods for synthesizing a wide range of ZIFs. We then review the crystal structure of ZIFs and describe the relationship between their structure and properties using an in-depth analysis. We also discuss several important and intrinsic features that make ZIFs stand out from MOFs and discrete molecular cages. Finally, we outline the future direction for this class of porous crystals.

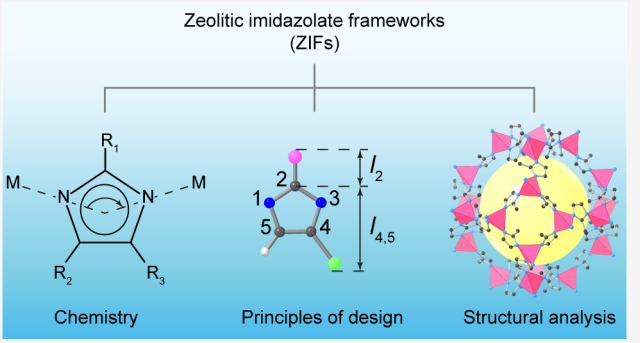

1. INTRODUCTION

Reticular chemistry, linking molecular building units through strong bonds into crystalline extended structures, has resulted in metal−organic frameworks (MOFs), covalent organic frameworks (COFs), and zeolitic imidazolate frameworks (ZIFs).[1−5] These are being made and studied in many applications including climate change.[6−8] ZIFs stand out for their zeolite-like structures in which conceptually the Si−O−Si fragment in zeolites (Figure 1a) is replaced by M−L−M (where M is tetrahedral metal ions such as Zn, Co, Cd, Cu, and Fe and L is an imidazolate linker).[9−11] The preferred angle around the oxygen in zeolites is 145°, matching closely with the corresponding angle of a bridging imidazolate (Figure 1b) in ZIF structures (Figure 1c).[12−15] This idea was put into practice, resulting in more than 100 new ZIFs (Table 1 and Supporting Information, SI, Figures S1 and S2).[16−22] In addition to structures known in zeolites, new tetrahedral topologies have been achieved in ZIFs.[12,17,21] It must be noted that certain topologies of zeolites have not yet been found in ZIFs.[9,23]

In this contribution, we discuss a general synthetic strategy used for uncovering the vast structure space of ZIFs and highlight the fundamental differences between the MOFs and ZIFs. Specifically, the mixed linker approach gives rise to making ZIFs with large apertures and cavities as well as accessing new topologies. We also elucidate the unique pore metrics and linker flexibility of ZIFs that impart their exceptional chemical and thermal stability. In addition, we show how ZIFs are a special subclass of MOFs because small linkers are used to make very large pore openings and cavities. The fact that the structures of ZIFs are intrinsically reticulated solid-state cages in three dimensions offers an alternative to molecular cages, the chemistry of which is complicated by their Brownian motion in solution. This allows for enhanced control of the chemical structure, enabling confinement in the pores without solvent interference.

2. ZIFS VERSUS MOLECULAR CAGES

In considering ZIF structures, it is crucial to understand their distinction from similar crystalline solids. In ZIFs, the metal ions serve as nodes that are connected by imidazole-based linkers to form a three-dimensional framework.[12] ZIFs have a high degree of tunability in their structures and properties due to the ability to vary connection of metal ions and linkers used in their synthesis, and they have shown great potential in applications such as gas storage, separation, and sensing.[10,48−51] Metal−organic molecular cages (MOCs), on the other hand, are discrete, self-assembled structures made up of organic linkers and metal ions that form a cage-like structure around a central cavity.[52−55] The behavior of these cages in solution is dominated by Brownian motion, the random movement of particles in a fluid due to their collisions with other fast-moving molecules in the solution. This characteristic

Received: July 8, 2023
Revised: November 20, 2023
Accepted: November 22, 2023
Published: December 8, 2023

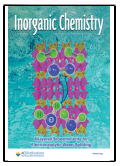

https://doi.org/10.1021/acs.inorgchem.3c02322
Inorg. Chem. 2023, 62, 20861−20873

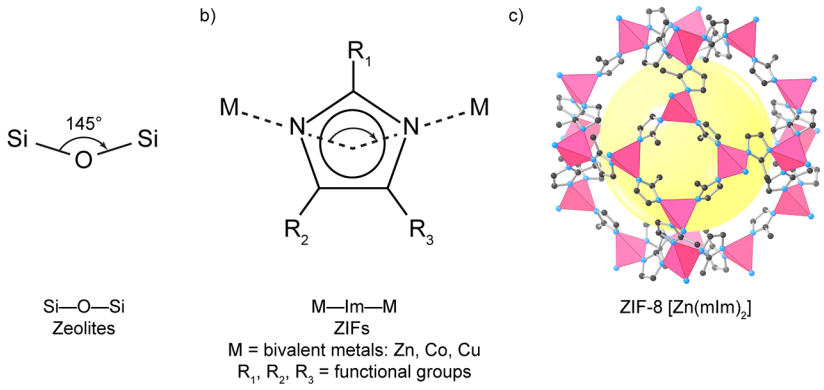

Figure 1. (a) Bridging angle (145°) of Si−O−Si in zeolites. (b) The M−Im−M in ZIFs, which is a requisite for synthesizing zeolite-type structures, as presented in ZIF-8 structure [$Zn(mIm)_2$] (mIm = 2-methylimidazolate). (c) Crystal structure of ZIF-8 viewed from the outside of the *t-toc* cage. Color code: Zn, pink; C, black; N, blue. H atoms are omitted for clarity.

can be coupled with their structural design to selectively capture and release guest molecules based on the size, shape, and polarity of the cavity and linkers used. Thus, MOCs have demonstrated promising applications in areas such as drug delivery, catalysis, and gas separation.[54,55]

The main difference between ZIFs and MOCs lies in their structure. While ZIFs have a continuous, interconnected framework with well-defined pores, molecular cages are discrete, self-assembled structures with a central cavity. ZIFs are generally larger in size and have a higher degree of porosity, which makes them well-suited for applications that require large surface areas and high gas uptake capacities. In contrast, MOCs are typically smaller in size and are designed to selectively capture and release specific guest molecules.[56,57]

ZIFs are designed based on reticular chemistry principles.[23] They consist of metal ions that serve as nodes or vertices, connected by organic linkers or edges, forming neutral, extended structures with well-defined pores. The metal ions in ZIFs adopt a tetrahedral geometry and are stitched with imidazolate units, producing zeolite-like structures. Furthermore, the flexibility of linkers and metals allows for the creation of nonzeolitic topologies.[21,25,28−32,43,47] In contrast, MOCs are designed based on the principles of supramolecular chemistry, using edge-sharing molecular polygons as discrete molecular entities. This means that the vertices in MOCs are not allowed to expand further. For the vertices in discrete cages to not link to each other (i.e., to form extended structures or MOFs), at least one organic linker that has a bent structure with the angle between two coordination sites less than 180° must be used.[9] Most MOCs are anionic compounds, except for those consisting of metal paddle wheels [$M_2(COO)_4$, M = Cu, Mo] and bent organic linkers.[55,58,59]

3. METHODS TO SYNTHESIZE VARIOUS ZIF TOPOLOGIES

The synthesis of ZIFs with various structure types (i.e., topologies) has been a focus since the beginning of the study of this class of reticular frameworks. Even now, this remains a priority in ZIF chemistry, as it has yet to be fully understood under which conditions novel ZIF topologies can crystallize. Discovering new ZIFs with novel topologies is challenging and often relies on trial-and-error experiments.[9,12,13,17,60] In this section, we summarize, highlight, and discuss different strategies reported in the literature for synthesizing new ZIFs, including the use of functionalized linkers, mixed linkers, and adjusting geometry based on mixed linkers. We aim to provide a clear picture of how to create new ZIFs.

One of the first examples of using the strategy that relies on a functionalized imidazole (Im) linker to vary the zeolite-like topology was reported in 2006.[14] The authors hypothesized that imidazole linkers with substituents at the 2-position could react with Zn^{2+} ions to form ZIFs bearing zeolite topologies. In their work, sod was formed when 2-methylimidazole (mIm) was used in the reaction with Zn^{2+} units, while ZIF with ana topology was obtained if 2-ethylimidazole (2eIm) was used. Upon close examination of the orientation of the functional groups in the two ZIFs, it was found that the methyl and ethyl groups affected the orientation of the Zn tetrahedral coordination, leading to a significant change in the interconnection between Zn atoms in the entire framework.

Early work on ZIFs, however, was limited by the fact that the principles of design were not fully understood, and detailed properties such as chemical stability and applicability were not studied.[13,14] Later, a series of ZIFs was made based on the analogy to zeolites.[12] It was discovered that ZIF-7 and ZIF-11, sharing the same composition $Zn(bIm)_2$ but different topologies (ZIF-7, sod; ZIF-11, rho), were obtained under two distinct synthetic conditions. Later on, a unique strategy for synthesizing important and large cage lta ZIFs was reported.[61] Particularly, replacing the C atom(s) at position 5 or positions 5 and 7 with N atom(s) in the linker led to the successful synthesis of ZIF-20 [$Zn(Pur)_2$, Pur = purine], ZIF-21 [$Co(Pur)_2$], and ZIF-22 [$Zn(5abIm)_2$, 5abIm = 5-azabenzimidazolate].

As demonstrated in the synthesis of LTA zeolites,[62] the initial formation of the cube played a critical role. The authors speculated that functionalizing bIm at 5 or 5 and 7 positions using N atoms resulted in a favorable proximity between the six-membered rings of two adjacent linkers. The CH−N···N−CH pair at positions 5 and 6 of the two linkers caused an electrostatic interaction and a dipole−dipole interaction, which in turn facilitated the formation of the cube (double-4-membered ring, *t-cub*; Figure 2a). According to the zeolite library,[63] LTA or ACO topology would be the default formation to link these cubes. However, ACO is unfavorable due to the large distortion of the Zn−N−N−Zn dihedral angles. Therefore, ZIFs with lta topology were dominantly produced. The dipole−dipole interaction was also found in six-membered and eight-membered rings in the lta ZIFs (Figure 2b,c). In contrast, the dipole−dipole interaction did not exist

https://doi.org/10.1021/acs.inorgchem.3c02322
Inorg. Chem. 2023, 62, 20861−20873

Table 1. Composition, CCDC Code, Topology Parameters, and Calculated Surface Area of Reported ZIFs[a]

common name	composition[b]	CCDC code	ZIF topology[c]	zeolite code	T/V [nm^{-3}][d]	D_i [Å][e]	D_f [Å][f]	surface area [m^2/g][g]	ref
ZIF-1	$Zn(Im)_2$	VEJYEP	**crb**	**BCT**	3.64	6.50	2.19	639	12
ZIF-2	$Zn(Im)_2$	VEJYIT	**crb**	**BCT**	2.80	6.42	5.29	1903	12
ZIF-3	$Zn(Im)_2$	VEJYOZ	**dft**	*h*	2.66	8.47	5.70	2083	12
ZIF-4	$Zn(Im)_2$	VEJYUF	**cag**	*h*	3.68	4.74	2.41	331	12
ZIF-5	$Zn_3In_2(Im)_{12}$	VEJZAM	**gar**	*h*	3.78	3.87	2.15	37	12
ZIF-6	$Zn(Im)_2$	EQOCOC	**gis**	**GIS**	4.73	4.83	1.64	51	12
ZIF-7	$Zn(bIm)_2$	VELVIS	**sod**	**SOD**	2.50	5.59	2.40	288	12
ZIF-8	$Zn(mIm)_2$	VELVOY	**sod**	**SOD**	2.45	11.39	3.41	1410	12
ZIF-9	$Co(bIm)_2$	VEJZEQ	**sod**	**SOD**	2.51	5.64	2.46	294	12
ZIF-10	$Zn(Im)_2$	VEJZIU	**mer**	**MER**	2.25	12.35	7.49	2334	12
ZIF-11	$Zn(bIm)_2$·	VEJZOA	**rho**	**RHO**	2.02	14.86	2.46	928	12
ZIF-12	$Co(bIm)_2$	VEJZUG	**rho**	**RHO**	2.02	14.91	2.46	1044	12
ZIF-14	$Zn(eIm)_2$	MECWIB	**ana**	**ANA**	2.57	6.06	4.27	744	14
ZIF-20	$Zn(Pur)_2$	MIHHAN	**lta**	**LTA**	2.04	15.45	2.87	1108	16
ZIF-21	$Co(Pur)_2$	MIHHER	**lta**	**LTA**	2.04	15.50	2.86	1114	16
ZIF-22	$Zn(5abIm)_2$	MIHHIV	**lta**	**LTA**	2.02	15.30	2.89	1064	16
ZIF-23	$Zn(4abIm)_2$	MIHHOB	**dia**	N/A	3.32	2.24	1.43	0	16
ZIF-25	$Zn(dmbIm)_2$	POVNIA	**rho**	**RHO**	2.20	16.80	4.76	1023[i]	18
ZIF-60	$Zn_2(Im)_3(mIm)$	GITSUY	**mer**	**MER**	2.24	12.38	7.61	2265	17
ZIF-61	$Zn(Im)(mIm)$	GITTAF	**zni**	*h*	4.62	2.38	1.25	0	17
ZIF-62	$Zn(Im)_{1.75}(bIm)_{0.25}$	GIZJOP	**cag**	*h*	3.58	5.30	1.66	279	17
ZIF-64	$Zn(Im)_2$	GITTEJ	**crb**	**BCT**	3.62	6.39	2.15	675	17
ZIF-65	$Co(nIm)_2$	GITTIN	**sod**	**SOD**	2.33	11.24	3.73	1210	17
ZIF-67	$Co(mIm)_2$	GITTOT	**sod**	**SOD**	2.46	11.41	3.34	1439	17
ZIF-68	$Zn(bIm)(nIm)$	GITTUZ	**gme**	**GME**	2.12	10.86	8.04	1192	17
ZIF-69	$Zn(cbIm)(nIm)$	GITVAH	**gme**	**GME**	2.10	8.76	4.92	579	17
ZIF-70	$Zn(Im)_{1.13}(nIm)_{0.87}$	GITVEL	**gme**	**GME**	2.11	14.46	13.38	1686	17
ZIF-71	$Zn(dcIm)_2$	GITVIP	**rho**	**RHO**	2.06	17.02	5.46	847	17
ZIF-72	$Zn(dcIm)_2$	GIZJUV	**lcs**	*h*	3.16	3.14	1.97	0	17
ZIF-73	$Zn(nIm)_{1.74}(mbIm)_{0.26}$	GITVOV	**frl**	*h*	3.20	5.38	1.34	133	17
ZIF-74	$Zn(mbIm)(nIm)$	GITVUB	**gis**	**GIS**	2.67	4.25	1.77	67	17
ZIF-75	$Co(mbIm)(nIm)$	GITWAI	**gis**	**GIS**	2.67	4.29	1.77	83	17
ZIF-76	$Zn(Im)(cbIm)$	GITWEM	**lta**	**LTA**	2.07	11.86	2.82	754	17
ZIF-77	$Zn(nIm)_2$	GITWIQ	**frl**	*h*	3.23	5.05	3.97	444	17
ZIF-78	$Zn(nbIm)(nIm)$	YOZBIZ	**gme**	**GME**	25.01	7.40	4.52	41	19
ZIF-79	$Zn(mbIm)(nIm)$	YOZBOF	**gme**	**GME**	25.26	7.89	4.45	59	19
ZIF-80	$Zn(dcIm)(nIm)$	YOZBUL	**gme**	**GME**	24.82	12.17	10.29	101	19
ZIF-81	$Zn(brbIm)(nIm)$	YOZCAS	**gme**	**GME**	24.99	8.43	4.31	65	19
ZIF-82	$Zn(cyIm)(nIm)$	YOZCEW	**gme**	**GME**	25.07	11.77	10.12	108	19
ZIF-90	$Zn(alIm)_2$	WOJGEI	**sod**	**SOD**	2.33	11.01	3.49	1320	20
ZIF-91	$Zn(hmIm)_2$	*j*	**sod**	**SOD**	31.63	9.08	3.33	41	20
ZIF-92	$Zn(heIm)_2$	*j*	**sod**	**SOD**	31.78	3.62	1.12	0	20
ZIF-93	$Zn(4m5alIm)_2$	POVNEW	**rho**	**RHO**	2.95	14.93	3.25	391	18
ZIF-95	$Zn(cbIm)_2$	NOFQAB	**poz**	*h*	1.51	21.10	4.63	1208	21
ZIF-96	$Zn(4cy5amIm)_2$	POVNOG	**rho**	**RHO**	2.76	16.08	4.97	817	18
ZIF-97	$Zn(4hm5mIm)_2$	POVNAS	**rho**	**RHO**	2.74	15.45	2.93	450	18
ZIF-100	$Zn_{20}(cbIm)_{39}$	NOFQEF	**moz**	*h*	1.29	35.57	4.79	1641	21
ZIF-300	$Zn(mIm)_{0.86}(brbIm)_{1.14}$	TOHDAX	**cha**	**CHA**	2.39	7.20	4.55	272	24
ZIF-301	$Zn(mIm)_{0.94}(cbIm)_{1.06}$	TOHDEB	**cha**	**CHA**	2.49	7.23	4.59	297	24
ZIF-302	$Zn(mIm)_{0.67}(mbIm)_{1.33}$	TOHDIF	**cha**	**CHA**	2.37	7.96	4.38	441	24
ZIF-303	$Zn(cbIm)_{0.7}(nIm)_{0.3}(Im)$	NEHLOE	**cha**	**CHA**	2.14	8.55	4.67	1082	25
ZIF-318	$Zn(mIm)(tfmIm)$	DEBXUG	**sod**	**SOD**	2.41	10.65	3.50	1070	26
ZIF-360	$Zn(bIm)(nIm)_{0.7}(Im)_{0.3}$	NEHLUK	**kfi**	**KFI**	2.07	15.92	5.46	1294	25
ZIF-365	$Zn(cbIm)_{0.95}(nIm)_{0.60}(Im)_{0.45}$	NEHMAR	**kfi**	**KFI**	2.10	12.99	4.70	1067	25
ZIF-376	$Zn(nbIm)_{0.25}(mIm)_{0.25}(Im)_{1.5}$	NEHMEV	**lta**	**LTA**	2.05	10.31	4.48	1124	25
ZIF-386	$Zn(nbIm)_{0.85}(nIm)_{0.7}(Im)_{0.45}$	NEHMIZ	**afx**	**AFX**	2.19	9.27	4.68	911	25
ZIF-408	$Zn(cbIm)_{1.86}(mIm)_{0.09}$	NEHMOF	**moz**	*h*	1.36	33.73	4.54	1541	25
ZIF-410	$Zn(cbIm)_{1.1}(alIm)_{0.9}$	NEHMUL	**gme**	**GME**	2.11	8.25	4.92	1002	25
ZIF-412	$Zn(bIm)_{1.13}(nIm)_{0.62}(Im)_{0.25}$	NEHNAS	**ucb**	*h*	1.53	33.67	8.49	1680	25
ZIF-413	$Zn(mbIm)_{1.03}(nIm)_{0.64}(Im)_{0.33}$	NEHKET	**ucb**	*h*	1.52	31.26	5.99	1665	25

https://doi.org/10.1021/acs.inorgchem.3c02322
Inorg. Chem. 2023, 62, 20861−20873

Table 1. continued

common name	composition[b]	CCDC code	ZIF topology[c]	zeolite code	T/V [nm^{-3}][d]	D_i [Å][e]	D_f [Å][f]	surface area [m^2/g][g]	ref
ZIF-414	$Zn(nbIm)_{0.91}(mIm)_{0.62}(Im)_{0.47}$	NEHKIX	**ucb**	*h*	1.53	30.80	5.39	1720	25
ZIF-486	$Zn(nbIm)_{0.2}(mIm)_{0.65}(Im)_{1.15}$	NEHKOD	**gme**	**GME**	2.25	8.54	5.49	1738	25
ZIF-516	$Zn(mbIm)_{1.23}(brbIm)_{0.77}$	NEHKUJ	**ykh**	*h*	1.75	7.43	3.92	719	25
ZIF-586	Zn(mbIm)(2mbIm)	NEHLAQ	**ykh**	*h*	1.70	11.46	7.66	1334	25
ZIF-615	Zn(cbIm)(4nIm)	NEHLEU	**gcc**	*h*	1.94	15.59	14.30	893	25
ZIF-725	$Zn(brbIm)_{1.35}(nIm)_{0.4}(Im)_{0.25}$	NEHLIY	**bam**	*h*	1.54	23.96	21.69	964	25
ZIF-1001	$Zn_3(bTZ)_{4.5}(bIm)_{1.5}$	KEJCOV	**npo**	**NPO**	2.76	4.85	3.53	192	27
ZIF-1002	$Zn_3(bTZ)_{4.8}(mbIm)_{1.2}$	KEJCUB	**npo**	**NPO**	2.75	4.17	2.29	34	27
ZIF-1003	$Zn_3(bTZ)_{4.8}(brbIm)_{1.2}$	KEJDEM	**npo**	**NPO**	2.74	4.24	2.50	73	27
ZIF-1004	$Zn_3(bTZ)_{4.91}(cbIm)_{1.09}$	KEJDAI	**npo**	**NPO**	2.74	4.50	2.91	123	27
ZIF-CO3−1	$Zn_2(mIm)_2(CO_3)$	HOYQAP	**mog**	*h*	6.62	2.85	1.25	0	28
ZIF-coi	$Zn(Im)_2$	EQOCOC	**coi**	*h*	4.73	4.83	1.64	51	29
ZIF-neb	$Zn(Im)_2$	KEVLEE	**neb**	*h*	3.89	4.38	2.33	340	30
ZIF-nog	$Zn(Im)_2$	HICGEG	**nog**	*h*	2.96	7.37	4.99	1656	31
ZIF-ana	$Zn(pIm)_2$	GUPFAZ	**ana**	**ANA**	2.59	4.27	2.97	33	32
ZIF-UC-1	$Zn(Im)_{1.6}(bIm)_{0.21}(mbIm)_{0.19}$	RUFQAN	**cag**	*h*	3.45	3.21	1.54	0	33
ZIF-UC-2	$Zn(Im)_{1.87}(5f6cbIm)_{0.13}$	GULVAN	**cag**	*h*	3.64	3.29	1.95	0	34
ZIF-UC-3	$Zn(Im)_{1.81}(2m5cbIm)_{0.19}$	GULVER	**cag**	*h*	3.43	5.18	1.88	345	34
ZIF-UC-4	$Zn(Im)_{1.66}(5fbIm)_{0.34}$	GULVOB	**cag**	*h*	3.56	3.08	1.54	0	34
ZIF-UC-5	$Zn(Im)_{1.72}(cbIm)_{0.28}$	GULVIV	**cag**	*h*	3.49	2.85	1.48	0	34
ZIF-UC-6	$Zn(Im)_{1.82}(abIm)_{0.18}$	PAYBEA	**cag**	*h*	3.60	2.85	1.48	0	35
ZIF-UC-7	$Zn(Im)_{1.75}(Pur)_{0.25}$	ZIBVIT	**cag**	*h*	3.71	5.18	1.41	289	36
ZIF-4-CN	$Zn(Im)_{1.82}(cyIm)_{0.18}$	BINNIZ	**cag**	*h*	3.74	4.51	1.58	214	37
Co-ZIF-68	Co(bIm)(nIm)	RIRDAZ	**gme**	**GME**	2.11	10.88	8.28	1238	38
Co-ZIF-69	Co(cbIm)(nIm)	RIRDED	**gme**	**GME**	2.07	8.70	4.93	1021	38
Co-ZIF-81	Co(brbIm)(nIm)	RIRDIH	**gme**	**GME**	2.07	8.40	4.41	841	38
CdIF-1	$Cd(mIm)_2$	GUPBUP	**sod**	**SOD**	2.02	12.69	4.01	1622	32
CdIF-4	$Cd(eIm)_2$	GUPCEA	**mer**	**MER**	1.63	20.62	7.96	1698	32
CdIF-5	$Cd(mIm)_2$	GUPCIE	**ict**	*h*	3.37	5.55	3.88	230	32
CdIF-6	$Cd(eIm)_2$	GUPCOK	**ana**	**ANA**	2.19	7.33	4.70	1008	32
CdIF-9	$Cd(nIm)_2$	GUPDEB	**rho**	**RHO**	1.69	20.69	7.65	1562	32
CdIF-10	$Cd(pIm)_2$	GUPDIF	**ana**	**ANA**	2.18	4.75	3.85	375	32
CdIF-12	$Cd(bIm)_2$	GUPDUR	**dia**	*h*	2.42	2.67	1.27	0	32
MUV-3	$Fe(mIm)_2$	RODLUU	**sod**	**SOD**	2.37	11.63	3.42	698	39
MUV-3- mimb	$Fe(mIm)_{1.5}(2mbIm)_{0.5}$	WASDED	**sod**	**SOD**	2.37	7.91	2.02	356	40
MUV-3-eimb	$Fe(eIm)_{1.34}(2mbIm)_{0.66}$	WASDIH	**sod**	**SOD**	2.31	7.93	0.34	397	40
MUV-6	$Fe(eIm)_2$	RODMOP	**qtz**	*h*	3.70	2.02	1.11	0	39
MUV-7	$Fe(2mbIm)_2$	RODMUV	**dia**	*h*	2.90	2.63	1.01	0	39
MUV-24-coi	$Fe(Im)_2$	OGELOF	**coi**	*h*	4.71	4.66	1.57	37	41
MUV-24-lla	$Fe(Im)_2$	OGELUL	*lla1*	*h*	4.90	2.69	1.41	0	41
TIF-1-Zn	$Zn(dmbIm)_2$	QOGPIM	**zea**	*h*	1.61	12.26	5.29	955	42
TIF-2	$Zn(Im)_{1.1}(mbIm)_{0.9}$	QOSXOM	**zeb**	*h*	2.31	9.75	7.72	754	43
TIF-3	Zn(Im)(mbIm)	QOSXUS	**pcb**	**ACO**	2.77	5.37	4.03	205	43
TIF-4	$Zn(Im)_{1.5}(mbIm)_{0.5}$	QOSYAZ	**cag**	*h*	3.46	2.48	1.37	0	43
TIF-5-Zn	Zn(Im)(dmbIm)	QOSYIH	**gis**	**GIS**	2.66	5.56	2.10	405	43
TIF-5-Co	Co(Im)(dmbIm)	QOSYED	**gis**	**GIS**	2.70	5.63	2.10	395	43
ZTIF-1	Zn(mTZ)(eIm)	YORCEP	**sod**	**SOD**	2.46	9.40	3.64	613	44
ZTIF-2	Zn(mTZ)(pIm)	YORCIP	**rho**	**RHO**	1.90	17.05	8.25	1497	44
ZTIF-9	$Zn(eTZ)_{0.86}(mIm)_{1.14}$	QUDJEH	**sod**	**SOD**	2.44	10.02	3.59	616	45
ZTIF-10	$Zn(vTZ)_{0.63}(mIm)_{1.37}$	QUDJIL	**sod**	**SOD**	2.43	8.73	2.93	373	45
ZTIF-14	Zn(TZ)(dmbIm)	HORBOI	**gis**	**GIS**	2.73	4.93	2.16	253	46
ZTIF-15	Zn(mTZ)(dmbIm)	HORBUO	**gis**	**GIS**	2.74	*i*	*i*	0	46
MAF-6	Zn(mIm)(eIm)	IGOGOD	**rho**	**RHO**	1.91	*i*	*i*	0	14
MAF-7	$Zn(mtz)_2$	KEYROX	**sod**	**SOD**	2.44	11.24	3.70	1512	47
MAF-31	$Zn(mIm)_2$	OFERUN05	**dia**	*h*	4.21	2.40	1.57	0	47
MAF-32	$Zn(eIm)_2$	EHETER01	**qtz**	*h*	3.74	2.06	1.20	0	47
MAF-33	$Zn(etz)_2$	KEYSEO	**dia**	*h*	3.47	2.34	1.49	0	47

[a]More detailed information on each ZIF is provided in the Supporting Information. For a wider summary of ZIFs and general zeolite-like structures detailing their topology and porosity, please refer to refs 7−9. [b]Formula excluding guests. For linker abbreviations, please refer to Figures S1 and S2 in the Supporting Information. [c]For a description of topology symbols, see ref 23. [d]T/V is the density of metal atoms per unit volume. [e]D_i is the

https://doi.org/10.1021/acs.inorgchem.3c02322
Inorg. Chem. 2023, 62, 20861−20873

Table 1. continued

largest cavity diameter. [f]D_f is largest free sphere diameter. [g]Surface area (the sum of accessible and nonaccessible surface area) was calculated using Zeo++; for more information, see ref 22. [h]No zeolite code is available for these ZIFs due to their new topologies, which are not present in zeolites. [i]The structural parameters and/or surface area are not available for these ZIFs because the CIF file is incomplete. [j]For ZIF-91 and ZIF-92 reported in ref 20, no CCDC codes are available, and their structures were obtained through simulations. All disordered structures were modified using Materials Studio for calculations.

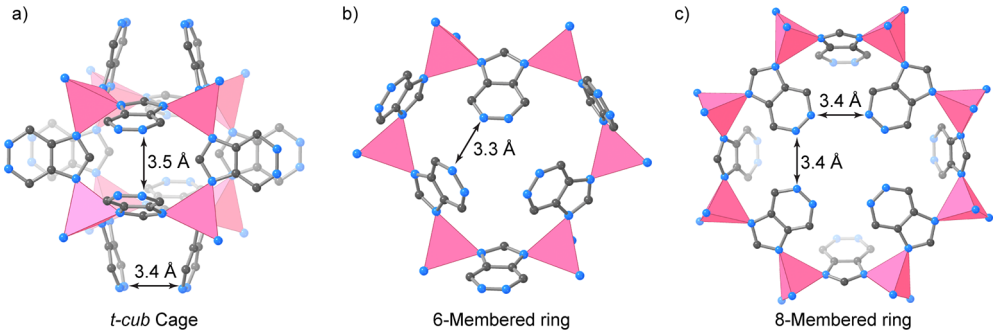

Figure 2. Dipole−dipole interaction of CH−N···N−CH pairs in the lta ZIF. Distances between two N atoms of the two linkers in (a) *t-cub*, (b) six-membered ring, and (c) eight-membered ring are in the range between 3.3 and 3.5 Å. We note that due to the disorder of nitrogen in the six-membered ring of 5abIm, two nitrogen atoms are shown. Color code: Zn, pink; C, black; N, blue. H atoms are omitted for clarity.

when bIm was functionalized with N at the 4 position. In other words, the linker(s) acted as a self-structure-directing agent through linker−linker interaction for the formation of ZIFs, representing another variant of the "structure-directing agent" approach in zeolite chemistry.

It is noted that ZIFs adopt tetrahedral structure types in which linkers are the primary units that can be adjusted. Consequently, one could change only the bulkiness, functionality, and flexibility of imidazole derivatives. To increase the complexity, from a topological perspective, increasing either the number of vertices (i.e., metal nodes) or edges (i.e., linkers), or even both, will expand the number of reticular structures generated. Based on the observed linker−linker interaction, the mixed-linker approach was deployed for the first time to increase the structural complexity of ZIFs.[17] This resulted in the creation of ZIFs with new topologies and complex pore compositions and structures. By mixing two linkers of different sizes, 10 mixed-linker ZIFs were created with the following topologies: mer [ZIF-60, Zn$(Im)_{1.5}(mIm)_{0.5}$], zni [ZIF-61, Zn(Im)(mIm)], cag [ZIF-62, Zn$(Im)_{1.75}(bIm)_{0.25}$], gme [ZIF-68, Zn(bIm)(nIm), nIm = 2-methylimidazolate; ZIF-69, Zn(cbIm)(nIm), cbIm = 5-chlorobenzimidazolate; and ZIF-70, Zn$(Im)_{1.13}(nIm)_{0.87}$], frl [ZIF-73, Zn$(nIm)_{1.74}(mbIm)_{0.26}$; mbIm = 5(6)-methylbenzimidazolate], gis [ZIF-74, Zn(nIm)(mbIm) and ZIF-75, Co(nIm)(mbIm)], and lta [ZIF-76, Zn(Im)(cbIm)]. Yet there is no specific rule that determines the outcome of ZIF topologies; for example, using a 3:1 ratio of mIm and Im yields mer, but a 1:1 ratio yields zni.

Although the full extent of topological control using this strategy at the time was not fully understood, this method is considered the most effective approach for discovering new structure types in ZIF chemistry.[26,38,43,44] Nevertheless, it is undeniable that mixed linker strategy provides precise control over the pore environment in cages of ZIFs, for example, the gme ZIF series.[19] For this series to be synthesized, nIm with a $-NO_2$ group at the 2 position is necessary. This may be due to the formation of a double six-membered ring (D6R) of the *t-hpr* cage by which nIm linkers occupy half of all six edges and connect the two six-membered rings. Half of all edges of D6R are functionalized with Im or bIm linkers, with their functional groups pointing toward the *t-kno* cage. By using various functionalized imidazole or bIm linkers and nIm, the authors can synthesize five ZIFs [ZIF-78, Zn(nbIm)(nIm); ZIF-79, Zn(mbIm)(nIm); ZIF-80, Zn(dcIm)(nIm); ZIF-81, Zn(brbIm)(nIm); and ZIF-82, Zn(cyIm)(nIm); nbIm = 5-nitrobenzimidazolate, mbIm = 5-methylbenzimidazolate, dcIm = 4,5-dichloroimidazolate, brbIm = 5-bromobenzimidazolate, cyIm = 4-cyanoimidazolate] with a wide range of pore metrics and functionalities.

Similar behavior was observed in the formation of cha ZIFs,[24] which are composed of a mixture of mIm and functionalized bIm linkers [ZIF-300, Zn$(mIm)_{0.86}(brbIm)_{1.14}$; ZIF-301, Zn$(mIm)_{0.94}(cbIm)_{1.06}$; and ZIF-302, Zn$(mIm)_{0.67}(mbIm)_{1.33}$]. Indeed, the less bulky functional group at the 2 position (i.e., mIm) facilitates the construction of the *t-hpr* cage by locating at the edges connecting the D6R. Specific positions in the *t-cha* cage, which are not the edge shared between *t-hpr* and *t-cha*, are occupied by functionalized bIm linkers.

In addition to using the bulky functionalized Im linker (e.g., eIm), tetrazole was also used in the mixed linker strategy to create new ZIFs.[44] However, this effort resulted in only the synthesis of sod (ZTIF-1, Zn(mTZ)(eIm), mTZ = 5-methyltetrazolate) and rho ZIFs (ZTIF-2, Zn(mTZ)(pIm), pIm = 2-propylimidazolate). It is important to understand the design principles of ZIFs and how to apply them in synthesis. In 2017, several principles were reported for designing various unseen ZIF topologies bearing large pore openings and cages.[25] After careful analysis of crystal structures of previously known ZIFs and those reported at the time, the authors hypothesized that functional groups at specific positions on Im linkers contribute to either repulsive or attractive interactions among the linkers. The formation of ZIFs is hard to predict, but the concept of a "steric index" can help explain the diversity of ZIF structures formed through the mixed linker strategy. The steric index, δ, is calculated by multiplying the van der Waals volume (V) of the linker by its l, which is the length of the functional groups (Figure 3a).

$$\delta = V \times l$$

https://doi.org/10.1021/acs.inorgchem.3c02322
Inorg. Chem. 2023, 62, 20861−20873

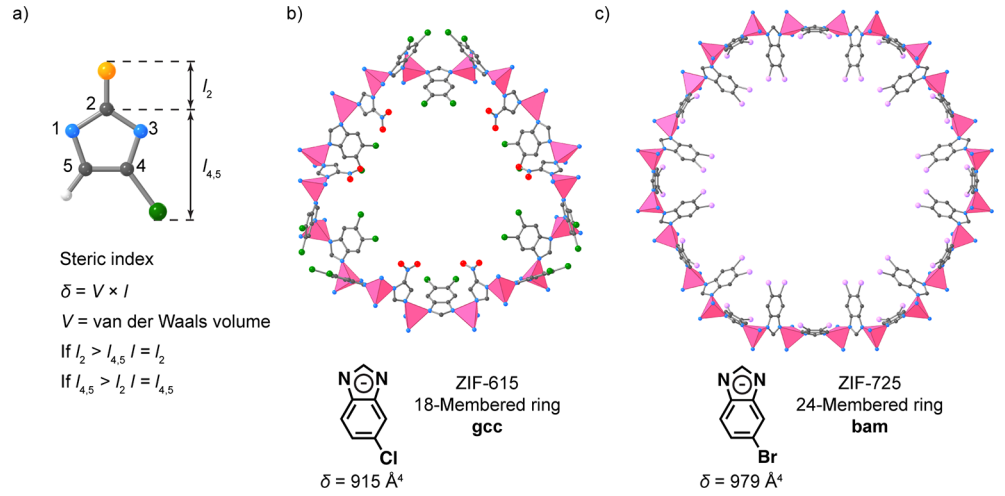

Figure 3. (a) Definition of the steric index, δ, and its equation. The δ is calculated for 5-chlorobenzimidazole and 5-bromoimidazole linkers, respectively. In the mixed-linker strategy, increasing the δ will increase the sizes of membered rings. (b) 18-membered ring in ZIF-615 and (c) 24-membered ring in ZIF-725. We note that due to the disorder of chlorine and bromine in the six-membered ring of cbIm and brbIm, respectively, two chlorine or bromine atoms are shown. Color code in ZIF-615 and ZIF-725: Zn, pink; C, black; N, blue; O, red; Cl, green; Br, purple. H atoms are omitted for clarity.

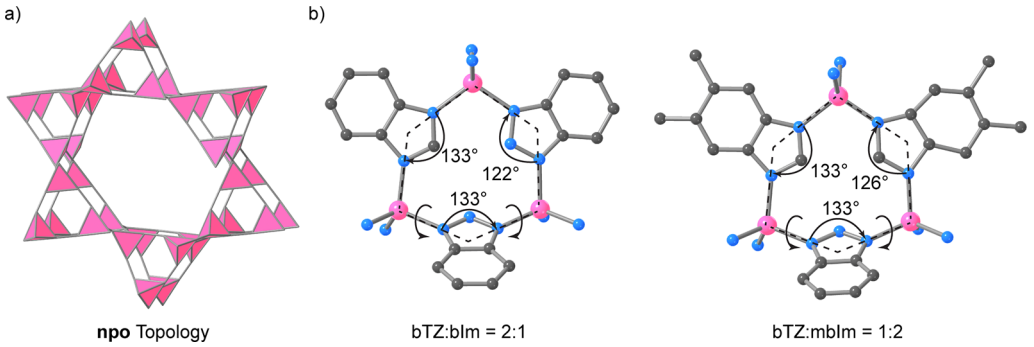

Figure 4. (a) Illustration of the NPO net. The npo ZIFs are produced by linking benzotriazole and functionalized benzimidazole linkers. (b) The formation of three-membered rings with angles of Zn−L−Zn are in the range between 122° and 133°. Color code: Zn, pink; C, black; N, blue. H atoms are omitted for clarity.

$$l = l_2 \text{ if } l_2 > l_{4,5}$$

$$l = l_{4,5} \text{ if } l_{4,5} > l_2$$

The steric index can be used to predict the pore openings and cage sizes in ZIFs. One design principle derived from the steric index is that the steric index determines the size of the opening with a greater steric index allowing for the formation of larger rings. For example, ZIF-615 [$Zn(cbIm)_{1.05}(4nIm)_{0.95}$, gcc topology] has a δ of 915 Å^4 and consists of 18-membered rings (as well as four-, six-, and eight-membered rings); ZIF-725 [$Zn(brbIm)_{1.35}(nIm)_{0.40}(Im)_{0.25}$, bam topology] has a δ of 979 Å^4 and consists of 24-membered rings (as well as four-, six-, and eight-membered rings; Figure 3b,c). Im linkers with the functional group at the 2 position tend to point into the small rings (usually four-membered ring). Im linkers with the functional groups at the four and five positions are more likely to point into eight-membered or larger rings. These functionalities at both specific positions can point into six-membered rings. As δ increases, larger membered rings can be formed, but it does not exclude the formation of smaller rings. In fact, combining many small δ Im linkers can hinder the formation of large-pore ZIFs. Larger pore openings and cages are made up of large and small rings, as seen in the two examples mentioned earlier. It is recommended to combine multiple Im linkers with various δ values, ranging from smaller to larger, to create ZIFs with large cage sizes. This principle is demonstrated through gme [ZIF-486, $Zn(nbIm)_{0.20}(mIm)_{0.65}(Im)_{1.15}$, 22.6 Å], gcc [ZIF-615, 27.2 Å], bam [ZIF-725, 39.0 Å], moz [ZIF-408, $Zn(cbIm)_{1.86}(mIm)_{0.09}(OH)_{0.05}$, 41.2 Å], and ucb [ZIF-412, $Zn(bIm)_{1.13}(nIm)_{0.62}(Im)_{0.25}$, 45.8 Å] ZIFs. The diversity of ZIFs also depends on the ability to vary the ratio of the Im linkers. The readers are additionally preferred to read the detailed description in the 2017 publication.[25] By changing the ratio of a given set of Im linkers, we can access many different structures. This allows further investigation of how to synthesize other ZIFs.

There is another way to diversify the ZIF structures, which relies on the modification of the M−L−M angle.[27] In particular, the geometry of M−L−M was adjusted using a mixed linker approach in which the main component must be benzotriazolate linker (bTZ). Reticulating bTZ and functionalized bIm in a ratio of 3:1 to 4.56:1 enabled the formation of smallest three-membered rings, which are crucial for the constructing of zeolite NPO net (Figure 4a). The authors found that bTZ plays a significant role in preserving the geometry of Ge−O−Ge connectivity in NPO zeolites, in which

https://doi.org/10.1021/acs.inorgchem.3c02322
Inorg. Chem. 2023, 62, 20861−20873

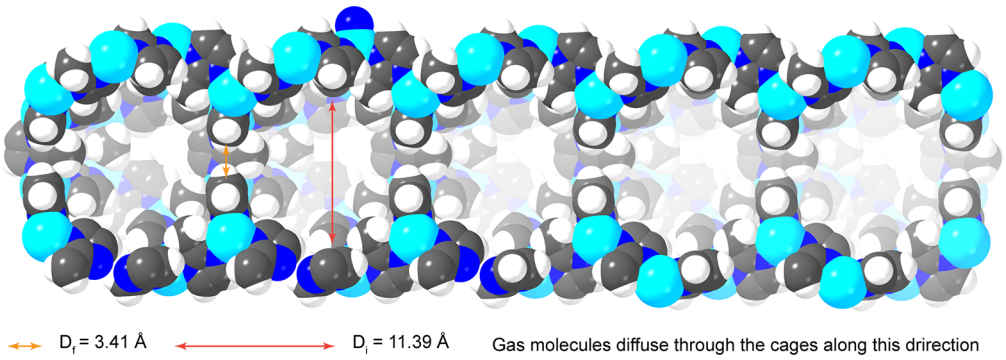

Figure 5. Demonstration of D_i and D_f in ZIF-8. The *t-toc* cages of ZIF-8 are replicated along the [111] axis and are connected through six-membered rings for gas diffusion. Color code: Zn, cyan; C, black; N, blue; H, white.

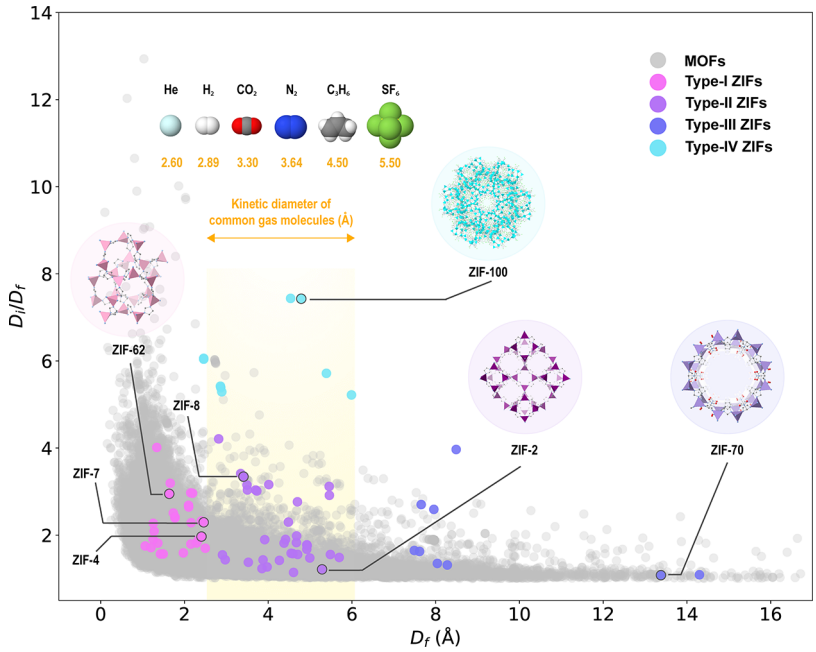

Figure 6. Scatterplot of D_i/D_f vs D_f of ZIFs and MOFs. The ZIFs are denoted in pink, purple, blue, and cyan, while the MOFs from the CSD MOF collection are denoted in gray. The range of kinetic diameters of common gas molecules is set from 2.6 to 6 Å, covering molecules from helium to sulfur hexafluoride. Four ZIFs representing the four types are distinguished.

the ∠(Ge−O−Ge) angle is around 130° (Figure 4b). In the presence of bTZ, adjacent Zn−Im bonds can rotate away from the plane of the three-membered ring (Figure 4b), allowing angles formed by lines intersecting the three-membered ring and bTZ or bIm (θ_1 and θ_2) to be close to zero. This causes Zn^{2+} centers to adopt a perfect tetrahedral shape. As a result, this geometry stabilizes and thus facilitates the formation of the NPO zeolite structure, which otherwise cannot be achieved with other nets. Interestingly, the construction is possible only with the use of a mixture of bTZ and bIm [ZIF-1001, $Zn(bTZ)_{1.5}(bIm)_{0.5}$], mbIm [ZIF-1002, $Zn(bTZ)_{1.6}(mbIm)_{0.4}$], brbIm [ZIF-1003, $Zn(bTZ)_{1.6}(brbIm)_{0.4}$], or cbIm [ZIF-1004, $Zn(bTZ)_{1.64}(cbIm)_{0.36}$]. Without the functionalized bIm linker, no npo ZIFs were obtained, indicating that the bIm linkers direct the preferential reticulation of the npo ZIFs.

4. STRUCTURE−PROPERTY RELATIONSHIP OF ZIFS

4.1. Pore Metrics of ZIFs. One of the most interesting characteristics of ZIFs is their unique pore environments. It has been mentioned above that the construction of ZIFs is inspired from zeolite, but new topologies that are unprecedented in zeolites have been made owing to the power of ZIF chemistry. Several important pore metrics should be emphasized when describing the porosity, which are the diameter of largest free sphere (D_f), the diameter of the largest included sphere (D_i), surface area, and pore volume. These metrics have been calculated and listed in Tables 1 and S1 for all of the ZIFs whose single crystal structures are available. D_f is the largest size of a probe molecule capable of entering the pores, also known as the pore limiting diameter (PLD), and the minimum internal diameter that the molecule can experience along the diffusion pathway (Figure 5); D_i is the largest cavity diameter (LCD) and is typically equal to the largest internal diameter along the diffusion pathway. However, in some cases, when D_i is larger than the largest internal diameter, the probe molecule is trapped in the pores of D_i. It cannot escape unless the structure decomposes, or the pore aperture changes due to the external stimuli.

In order to better visualize the two extreme cases of ZIF pores, we present the scatter plot of D_i/D_f versus D_f for the ZIFs along with a comparison of other MOF structures from

https://doi.org/10.1021/acs.inorgchem.3c02322
Inorg. Chem. 2023, 62, 20861−20873

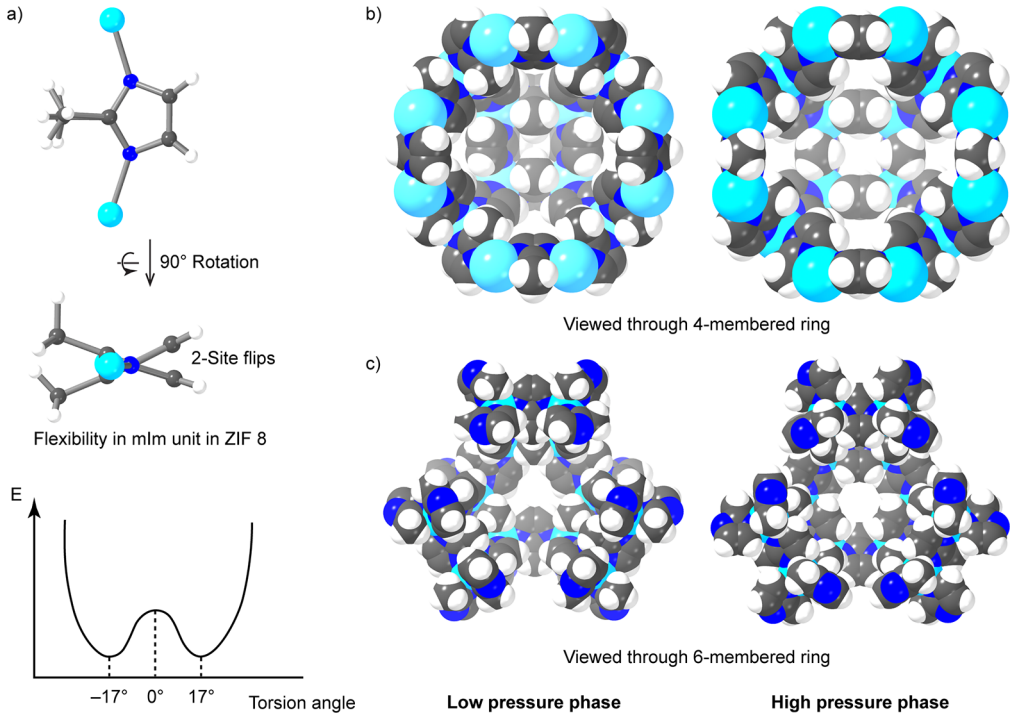

Figure 7. Illustration of the linker flexibility in ZIF-8 (sod). (a) The top and side view of the two-site flipping and libration of the mIm linker and the energy profile. (b) The view through the four-membered ring and the (c) six-membered ring of ZIF-8 at low and high pressure. Color code: Zn, cyan; C, black; N, blue; H, white.

the Cambridge Structural Database (CSD) MOF collection (Figure 6).[64] Based on the distribution of all the ZIF structures in Figure 6, we roughly classify the ZIFs into four categories. (1) Type-I ZIFs feature small D_f values (generally smaller than 2.6 Å, which is the kinetic diameter of helium, the smallest gas molecule) and therefore gas molecules normally cannot or are hard to get to enter the pores. (2) Type-II ZIFs have D_f values lying in the range of the kinetic diameters of common gas molecules (e.g., N_2, Ar, and CO_2). However, their D_i/D_f values are small, which means the gas molecules are diffusing in a pathway where there is a small variation of the internal diameter. (3) Type-III ZIFs have large D_f values (larger than 6 Å) corresponding to wide-open pore apertures, which allows all common gas molecules to freely diffuse. However, their D_i/D_f values are also close to one, which is consistent with the fact that ultralarge pores are thermodynamically unstable and therefore hard to be synthesized. (4) Type-IV ZIFs share comparable D_f values as Type-II ZIFs but have much larger D_i/D_f values (normally larger than 5), resulting in a great increase in both the surface area and the pore volume. The regions of the four types are also labeled in Figure 6.

The classification here based on the comparison between kinetic diameters and D_f values and the magnitude of D_i/D_f values is straightforward for knowing the variety in the pore metrics of ZIFs. However, it is important to note that the kinetic diameter does not provide a comprehensive assessment of the anisotropy and flexibility of guest molecules, nor does it account for the intricate interactions between guest molecules and the frameworks. Guest molecules having larger kinetic diameters than the D_f value of a ZIF may still be able to enter the pores considering the factors mentioned above. For a more rigorous analysis on the mechanism, it is essential to conduct simulation studies or in situ powder X-ray diffraction on prospective candidates that are near to the boundaries of our classification.[65]

4.2. Linker Flexibility in ZIFs. It should be noted that there are no strict boundaries between these four types of ZIFs as their structures have certain degrees of freedom that allow structural change such as the rotational dynamics of the Im linkers. Rotational dynamics is a general feature in MOFs as the void inside allows the organic moieties to rotate around the single bonds (e.g., the paraphenylene groups in terephthalates). However, the amplitude of such dynamics is restricted in ZIFs as a result of the nonlinear coordination geometry of the Im linkers. By using ^2H NMR techniques, it was found that there are multiple modes of rotation taking place in ZIFs involving the two-site hopping with fast liberation and swinging (Figure 7).[66] The former indicates that there are two energy minima sites for the linker position, which could also be identified from the positional disorder in the single crystal structures, whereas the swinging indicates a flatter potential energy profile within a wider range of rotation angles.

The rotational dynamics of the linkers create new possibilities for the interplay between the framework and the guests and therefore provide new insights beyond the static crystal structures. One of the well-studied examples is the pore aperture in ZIF-8. If the crystal structure obtained from the conventional single crystal X-ray diffraction experiment is used, the D_f of ZIF-8 is 3.41 Å, which is not available for nitrogen (kinetic diameter of 3.64 Å). However, two adsorption steps are observed in the semilog plot of the nitrogen isotherm, indicating a potential structural change that widens the pore aperture during the adsorption. This change was confirmed by simulating the N_2 adsorption process on the original single crystal structure as well as another ZIF-8 crystal structure obtained from high pressure diamond anvil cell experiments.[67] It was found that the linear structure of nitrogen also facilitates

https://doi.org/10.1021/acs.inorgchem.3c02322
Inorg. Chem. 2023, 62, 20861−20873

the reorientation of the linker by means of the efficient packing of nitrogen. Moreover, the rotational dynamics can be adjusted by the introduction of different functional groups. In another work, high-pressure powder X-ray diffraction, density functional theory, and grand canonical Monte Carlo simulation were performed for a series of sod ZIFs including ZIF-8, ZIF-90, and ZIF-65 with functional groups of increasing polarity ($-CH_3$, $-CHO$, and $-NO_2$) in the presence of methanol (kinetic diameter of 3.4 Å).[68] The results showed that a larger pore aperture is produced in the cases of the mIm and aIm linkers, while the nIm linkers rotate in the opposite direction, leading to a smaller pore aperture. In another sod ZIF, ZIF-7, linker-flexibility originated phase transition also takes place when guest molecules like DMF are introduced into or taken out from the pores.[69]

Linker flexibility is restricted to not only the sod ZIF mentioned above. Another well-known example is the cag ZIFs, including ZIF-4 and ZIF-62. In the case of ZIF-4, two distinct mechanisms (i.e., temperature and pressure) lead to an isotropic expansion or contraction of the crystal. In this process, the rotation of the linkers can go up to 69.3°.[70] Similarly, the linker-flexibility originated phase transition between an open-pore phase and a closed-pore phase was observed in ZIF-62 by in situ high-pressure X-ray diffraction.[71] The fraction of bIm in ZIF-62 can be altered to tune the threshold pressure for the phase transition.

4.3. Stability of ZIFs. As crystalline frameworks, ZIFs also exhibit exceptional thermal and chemical stability. The thermal stability is evaluated by finding the onset decomposition temperature from thermogravimetric experiments. Generally, ZIFs have an onset larger than 300 °C, and there are many ZIFs that are stable at 500 °C, owing to their chemical nature of reticulating metal cations with charged linkers to form a neutral framework. The chemical stability of the ZIFs was demonstrated by suspending the ZIF single crystals (ZIF-8 and ZIF-11) in solvents like benzene, methanol, water, and basic solution at multiple temperatures up to 1 week.[12] The crystals were examined by optical microscopy and powder X-ray diffraction, and no significant shape change or crystallinity loss were observed. The authors ascribed the exceptional chemical stability to the strong bonding between the Zn and N donors and the hydrophobic nature of the Im linkers, which prevent the tetrahedral building blocks from being attacked by solvent like water.

However, the chemical stability of ZIFs can also be measured by other metrics. Later studies found that some ZIFs slowly decompose in the water even at ambient conditions, and the metal ions and the Im linkers leaked into the water could form noncrystalline particles after the ZIFs are filtered and the water is evaporated.[72] At first glance, these results seem to be contradictory to what was previously observed, but it can be accounted for that the surfaces may have a different chemical environment compared to the interior of the ZIFs and therefore are more inclined to decompose. Indeed, studying the chemical stability of the ZIF surface is crucial to understanding their behavior, especially in the solution medium. However, the surface configuration is complicated as it is strongly correlated with synthetic or postsynthetic conditions. By using density functional theory and molecular dynamics, the surface phase diagram was constructed from a thermodynamics aspect for the (110) facet of ZIF-8 in gas phase and aqueous solution phase under different external parameters including temperature, pressure, and pH.[73] In the gas phase, the surface is quite stable, as it adopts a fully mIm terminated configuration. Whereas in the aqueous solution, pH was found to have a much stronger influence on the surface. Under a low pH environment where there are fewer unprotonated mIm linkers, the surface of ZIF-8 was found to have partial mIm terminated or total water/hydroxyl terminated, making it more vulnerable to decomposition.

4.4. Glassy Behavior of ZIFs. In view of the well-established porosity and structural tunability of ZIFs, it is conceptually possible to prepare ZIF glasses with permanent porosity through the thermally or pressure-induced amorphization of crystalline ZIFs.[74−77] This is possible since the transformation into denser and thermodynamically more stable phases is favored for the ZIFs in metastable phases.[9,78] In the presence of external stimuli,[79] when the melting occurs prior to decomposition, glassification takes place,[80,81] where metal retains their tetrahedra coordination geometry with distortion during the amorphization.[78,82,83] This results in the creation of a new class of ZIF derivatives through the melt-quenching route. The most noticeable change in this process is the decrease in order and the retention of the pores and short-range interactions. As a result, this new form of ZIF material is attractive to many applications due to (1) a large number of crystalline ZIFs with tunable composition and functionality prior to the melting and (2) enhancement of shaping ability, mass transport, and mechanical properties in the amorphous states.

For instance, when ZIF-4, $Zn(Im)_2$, was heated in an inert atmosphere, framework collapse at around 330 °C was observed.[78] Further heating at ∼450−500 °C resulted in the densification of the zni topology from the cag topology, which subsequently melted at around 575 °C. Quenching the liquid resulted in the creation of glassy ZIF-4, which has an identical composition to crystalline ZIF-4 but exhibits a glass transition behavior similar to silicate glasses upon reheating.[84] In addition to zinc-based ZIFs, such crystalline phase and topology transformations can also be observed in cobalt- and iron-based ZIF glasses.[75,85] It should be noted that the permanent porosity, processability, and shaping of such a material make it distinct from other melt-quenched glasses. For example, both ZIF-4 and another isostructural mixed-linker compound, ZIF-62, $Zn(Im)_{1.75}(bIM)_{0.25}$, have the cag topology.[33,34,37] It was found that the melting point of ZIF-62 was primarily affected by the presence of bulkier bIm linkers, and therefore adjusting the Im/bIm ratio in ZIF-62 can render the porous and tunable glassy ZIFs for gas separation.[75] Subsequent discoveries, such as the ZIF-UC family,[33−37] further highlighted the possibility of using a mixed-linker structure to produce cag topology ZIFs. This is achieved by replacing the bIm linker in ZIF-62 with differently functionalized bIm, leading to a variety of new ZIFs with altered thermal behaviors. Despite having nearly identical composition, the mechanical properties of glassy ZIFs have been examined and shown to be distinct from those of their crystalline counterparts.[86−89] These differences, including variations in toughness, strength, and hardness, as well as the inherent ability of glass to lack grain boundaries and have high processability, make it unique for mass transport and have potential for use in protective coatings and display technologies.[86]

https://doi.org/10.1021/acs.inorgchem.3c02322
Inorg. Chem. 2023, 62, 20861−20873

5. CONCLUDING REMARKS

ZIFs are a fascinating class of porous crystals because of their reticulated cage structures and tunable properties. The ability to diversify ZIF structures through the manipulation of linker chemistry and topologies has allowed for the creation of a wide range of crystalline solids. The linker−linker interaction and its use in the context of mixed-linkers impact the size of the pore opening and internal diameter and provide a powerful guide to accessing progressively larger pore ZIFs. In the future, more investigation is needed to completely grasp the mechanism of ZIF formation and establish guidelines for creating and synthesizing increasingly complex ZIFs. With such principles in hand, the in silico design of ZIFs with outstanding performance will be possible, and a deep understanding of the intricate relationship between the structure and properties, even for highly elaborate multinary structures, will be within reach. Additionally, the development of new computational and experimental techniques for probing the dynamic behavior of ZIFs will help shed light on the mechanisms behind their unique properties. The ability to tune the pore size and shape as well as the chemical stability of ZIFs will also be crucial for their practical use in a variety of fields.

On a fundamental level, ZIFs should be considered as reticulated cage structures in which such cages are pinned down in space and therefore potentially "addressable" through interaction with substrates occupying the pores. When compared to the structural properties of discrete metal−organic polyhedra, ZIFs stand out for their larger pore metrics, and when these properties are combined with their ordered structures, inclusion chemistry based on binding large biomolecules should be possible. As our understanding of ZIFs continues to deepen, it is likely that these materials will find even more widespread use in a variety of fields. Overall, the future looks bright for ZIFs, and we can expect to see continued progress and innovation in this field.

■ ASSOCIATED CONTENT

Supporting Information

The Supporting Information is available free of charge at https://pubs.acs.org/doi/10.1021/acs.inorgchem.3c02322.

Chemical structures and abbreviations of common linkers used in ZIF synthesis (PDF)

Detailed summary of the composition, CCDC code, topology, and sorption parameters of reported ZIFs (XLSX)

■ AUTHOR INFORMATION

Corresponding Author

Omar M. Yaghi − *Department of Chemistry, Kavli Energy Nanoscience Institute, and Bakar Institute of Digital Materials for the Planet, College of Computing, Data Science, and Society, University of California, Berkeley, California 94720, United States; KACST−UC Berkeley Center of Excellence for Nanomaterials for Clean Energy Applications, King Abdulaziz City for Science and Technology, Riyadh 11442, Saudi Arabia;* orcid.org/0000-0002-5611-3325; Email: yaghi@berkeley.edu

Authors

Zhiling Zheng − *Department of Chemistry, Kavli Energy Nanoscience Institute, and Bakar Institute of Digital Materials for the Planet, College of Computing, Data Science, and Society, University of California, Berkeley, California 94720, United States;* orcid.org/0000-0001-6090-2258

Zichao Rong − *Department of Chemistry, Kavli Energy Nanoscience Institute, and Bakar Institute of Digital Materials for the Planet, College of Computing, Data Science, and Society, University of California, Berkeley, California 94720, United States;* orcid.org/0000-0002-9014-9540

Ha L. Nguyen − *Department of Chemistry, Kavli Energy Nanoscience Institute, and Bakar Institute of Digital Materials for the Planet, College of Computing, Data Science, and Society, University of California, Berkeley, California 94720, United States;* orcid.org/0000-0002-4977-925X

Complete contact information is available at: https://pubs.acs.org/10.1021/acs.inorgchem.3c02322

Author Contributions

⊥These authors contributed equally. The manuscript was written through contributions of all authors. All authors have given approval to the final version of the manuscript.

Notes

The authors declare no competing financial interest.

Biographies

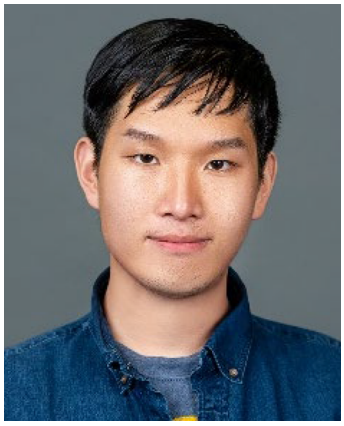

Zhiling Zheng received his Bachelor of Arts from Cornell University in 2019. He is currently pursuing his Ph.D. in chemistry under the supervision of Prof. Omar M. Yaghi at the University of California, Berkeley. His research interest focuses on the design and synthesis of new reticular materials and exploring the potential applications of artificial intelligence in the field of chemistry.

Zichao Rong obtained his B.Sc. degree with a major of Materials Chemistry at Peking University in 2020. Currently, he is a Ph.D. candidate in chemistry under the supervision of Prof. Omar M. Yaghi at University of California, Berkeley. His research interest lies in

https://doi.org/10.1021/acs.inorgchem.3c02322
Inorg. Chem. 2023, 62, 20861−20873

solving and analyzing the crystal structures of metal−organic frameworks (MOFs), correlating the latent features of MOF structures with the properties, and utilizing the power of data for synthesizing new MOFs as well as identifying the underlying crystallization mechanisms.

Dr. Nguyen obtained his Ph.D. in 2017 from the University of Technology, Vietnam National University Hochiminh (Vietnam). He spent almost a year working as a Research Consultant at King Fahd University of Petroleum and Minerals (Saudi Arabia). He then moved to the University of California Berkeley (United States) to work as a Postdoctoral Researcher in the group of Prof. Yaghi. Dr. Nguyen focuses his research on the design and synthesis of novel reticular materials (MOFs and COFs) for water sorption, CO_2 capture, and related energy applications.

Prof. Omar Yaghi obtained his Ph.D. from the University of Illinois—Urbana and was an NSF Postdoctoral Fellow at Harvard University. He currently holds the James and Neeltje Tretter Chair Professor of Chemistry at the University of California, Berkeley. He is the Chief Scientist of the Bakar Institute of Digital Materials for the Planet (BIDMaP) and the Co-Director of the Kavli Energy NanoScience Institute. He is well-known for establishing reticular chemistry and developing new classes of porous, crystalline solids, termed metal−organic frameworks and covalent organic frameworks.

■ ACKNOWLEDGMENTS

We are thankful for the financial support from Bakar Institute of Digital Materials for the Planet (BIDMaP) and Defense Advanced Research Projects Agency (DARPA). Z.Z. is thankful for the financial support through a Kavli ENSI Graduate Student Fellowship.

■ REFERENCES

(1) Yaghi, O. M. The reticular chemist. *Nano Lett.* **2020**, *20* (12), 8432−8434.
(2) Yaghi, O. M. Reticular chemistry: molecular precision in infinite 2D and 3D. *Mol. Front. J.* **2019**, *3* (01), 66−83.
(3) Yaghi, O. M.; O'Keeffe, M.; Ockwig, N. W.; Chae, H. K.; Eddaoudi, M.; Kim, J. Reticular synthesis and the design of new materials. *Nature* **2003**, *423* (6941), 705−714.
(4) Yaghi, O. M.; Kalmutzki, M. J.; Diercks, C. S. *Introduction to Reticular Chemistry: Metal-Organic Frameworks and Covalent Organic Frameworks*; John Wiley & Sons, 2019.
(5) Rungtaweevoranit, B.; Diercks, C. S.; Kalmutzki, M. J.; Yaghi, O. M. Spiers Memorial Lecture: Progress and prospects of reticular chemistry. *Faraday Discuss.* **2017**, *201*, 9−45.
(6) Yang, P.; Clark, D. S.; Yaghi, O. M. Envisioning the "Air Economy"—Powered by Reticular Chemistry and Sunlight for Clean Air, Clean Energy, and Clean Water. *Mol. Front. J.* **2021**, *5* (01n02), 30−37.
(7) Liu, C.-H.; Nguyen, H. L.; Yaghi, O. M. Harvesting Water from Desert Air. *AsiaChem. Mag.* **2020**, *1*, 18−25.
(8) Pimentel, B. R.; Parulkar, A.; Zhou, E. k.; Brunelli, N. A.; Lively, R. P. Zeolitic imidazolate frameworks: next-generation materials for energy-efficient gas separations. *ChemSusChem* **2014**, *7* (12), 3202−3240.
(9) Wang, H.; Pei, X.; Kalmutzki, M. J.; Yang, J.; Yaghi, O. M. Large Cages of Zeolitic Imidazolate Frameworks. *Acc. Chem. Res.* **2022**, *55* (5), 707−721.
(10) Phan, A.; Doonan, C. J.; Uribe-Romo, F. J.; Knobler, C. B.; O'keeffe, M.; Yaghi, O. M. Synthesis, structure, and carbon dioxide capture properties of zeolitic imidazolate frameworks. *Acc. Chem. Res.* **2010**, *43* (1), 58−67.
(11) Noh, K.; Lee, J.; Kim, J. Compositions and structures of zeolitic imidazolate frameworks. *Isr. J. Chem.* **2018**, *58* (9−10), 1075−1088.
(12) Park, K. S.; Ni, Z.; Côté, A. P.; Choi, J. Y.; Huang, R.; Uribe-Romo, F. J.; Chae, H. K.; O'Keeffe, M.; Yaghi, O. M. Exceptional chemical and thermal stability of zeolitic imidazolate frameworks. *Proc. Natl. Acad. Sci. U.S.A.* **2006**, *103* (27), 10186−10191.
(13) Huang, X.; Zhang, J.; Chen, X. [Zn (bim) 2]·(H2O) 1.67: A metal-organic open-framework with sodalite topology. *Chin. Sci. Bull.* **2003**, *48* (15), 1531−1534.
(14) Huang, X. C.; Lin, Y. Y.; Zhang, J. P.; Chen, X. M. Ligand-directed strategy for zeolite-type metal−organic frameworks: zinc (II) imidazolates with unusual zeolitic topologies. *Angew. Chem., Int. Ed.* **2006**, *45* (10), 1557−1559.
(15) Tan, J. C.; Bennett, T. D.; Cheetham, A. K. Chemical structure, network topology, and porosity effects on the mechanical properties of Zeolitic Imidazolate Frameworks. *Proc. Natl. Acad. Sci. U.S.A.* **2010**, *107* (22), 9938−9943.
(16) Pan, L.; Olson, D. H.; Ciemnolonski, L. R.; Heddy, R.; Li, J. Separation of hydrocarbons with a microporous metal−organic framework. *Angew. Chem., Int. Ed.* **2006**, *45* (4), 616−619.
(17) Banerjee, R.; Phan, A.; Wang, B.; Knobler, C.; Furukawa, H.; O'Keeffe, M.; Yaghi, O. M. High-throughput synthesis of zeolitic imidazolate frameworks and application to CO2 capture. *Science* **2008**, *319* (5865), 939−943.
(18) Morris, W.; Leung, B.; Furukawa, H.; Yaghi, O. K.; He, N.; Hayashi, H.; Houndonougbo, Y.; Asta, M.; Laird, B. B.; Yaghi, O. M. A combined experimental− computational investigation of carbon dioxide capture in a series of isoreticular zeolitic imidazolate frameworks. *J. Am. Chem. Soc.* **2010**, *132* (32), 11006−11008.
(19) Banerjee, R.; Furukawa, H.; Britt, D.; Knobler, C.; O'Keeffe, M.; Yaghi, O. M. Control of pore size and functionality in isoreticular zeolitic imidazolate frameworks and their carbon dioxide selective capture properties. *J. Am. Chem. Soc.* **2009**, *131* (11), 3875−3877.
(20) Morris, W.; Doonan, C. J.; Furukawa, H.; Banerjee, R.; Yaghi, O. M. Crystals as molecules: postsynthesis covalent functionalization of zeolitic imidazolate frameworks. *J. Am. Chem. Soc.* **2008**, *130* (38), 12626−12627.

https://doi.org/10.1021/acs.inorgchem.3c02322
Inorg. Chem. 2023, 62, 20861−20873

(21) Wang, B.; Côté, A. P.; Furukawa, H.; O'Keeffe, M.; Yaghi, O. M. Colossal cages in zeolitic imidazolate frameworks as selective carbon dioxide reservoirs. *Nature* **2008**, *453* (7192), 207−211.
(22) Martin, R. L.; Haranczyk, M. Construction and characterization of structure models of crystalline porous polymers. *Cryst. Growth Des.* **2014**, *14* (5), 2431−2440.
(23) O'Keeffe, M.; Peskov, M. A.; Ramsden, S. J.; Yaghi, O. M. The reticular chemistry structure resource (RCSR) database of, and symbols for, crystal nets. *Acc. Chem. Res.* **2008**, *41* (12), 1782−1789.
(24) Nguyen, N. T.; Furukawa, H.; Gándara, F.; Nguyen, H. T.; Cordova, K. E.; Yaghi, O. M. Selective capture of carbon dioxide under humid conditions by hydrophobic chabazite-type zeolitic imidazolate frameworks. *Angew. Chem.* **2014**, *126* (40), 10821−10824.
(25) Yang, J.; Zhang, Y.-B.; Liu, Q.; Trickett, C. A.; Gutiérrez-Puebla, E.; Monge, M. A.; Cong, H.; Aldossary, A.; Deng, H.; Yaghi, O. M. Principles of designing extra-large pore openings and cages in zeolitic imidazolate frameworks. *J. Am. Chem. Soc.* **2017**, *139* (18), 6448−6455.
(26) Mondal, S. S.; Hovestadt, M.; Dey, S.; Paula, C.; Glomb, S.; Kelling, A.; Schilde, U.; Janiak, C.; Hartmann, M.; Holdt, H.-J. Synthesis of a partially fluorinated ZIF-8 analog for ethane/ethene separation. *CrystEngComm* **2017**, *19* (39), 5882−5891.
(27) Zha, X.; Li, X.; Al-Omari, A. A.; Liu, S.; Liang, C.-C.; Al-Ghourani, A.; Abdellatief, M.; Yang, J.; Nguyen, H. L.; Al-Maythalony, B.; Shi, Z.; Cordova, K. E.; Zhang, Y.-B. Zeolite NPO-Type Azolate Frameworks. *Angew. Chem.* **2022**, *134* (39), e202207467.
(28) Basnayake, S. A.; Su, J.; Zou, X.; Balkus, K. J., Jr Carbonate-based zeolitic imidazolate framework for highly selective CO2 capture. *Inorg. Chem.* **2015**, *54* (4), 1816−1821.
(29) Tian, Y. Q.; Cai, C. X.; Ren, X. M.; Duan, C. Y.; Xu, Y.; Gao, S.; You, X. Z. The Silica-Like Extended Polymorphism of Cobalt (II) Imidazolate Three-Dimensional Frameworks: X-ray Single-Crystal Structures and Magnetic Properties. *Eur. J. Chem.* **2003**, *9* (22), 5673−5685.
(30) Schröder, C. A.; Saha, S.; Huber, K.; Leoni, S.; Wiebcke, M. Metastable metal imidazolates: development of targeted syntheses by combining experimental and theoretical investigations of the formation mechanisms. *Z. fur Krist. - Cryst. Mater.* **2014**, *229* (12), 807−822.
(31) Koyama, Y.; Ikeda, T.; Tatsumi, T.; Kubota, Y. A Multi-Dimensional Microporous Silicate That Is Isomorphous to Zeolite MCM-68. *Angew. Chem., Int. Ed.* **2008**, *47* (6), 1042−1046.
(32) Tian, Y. Q.; Yao, S. Y.; Gu, D.; Cui, K. H.; Guo, D. W.; Zhang, G.; Chen, Z. X.; Zhao, D. Y. Cadmium imidazolate frameworks with polymorphism, high thermal stability, and a large surface area. *Eur. J. Chem.* **2010**, *16* (4), 1137−1141.
(33) Rios Gómez, M. L.; Lampronti, G. I.; Yang, Y.; Mauro, J. C.; Bennett, T. D. Relating structural disorder and melting in complex mixed ligand zeolitic imidazolate framework glasses. *Dalton Trans.* **2020**, *49* (3), 850−857.
(34) Hou, J.; Rios Gomez, M. L.; Krajnc, A.; McCaul, A.; Li, S.; Bumstead, A. M.; Sapnik, A. F.; Deng, Z.; Lin, R.; Chater, P. A.; Keeble, D. S.; Keen, D. A.; Appadoo, D.; Chan, B.; Chen, V.; Mali, G.; Bennett, T. D. Halogenated metal−organic framework glasses and liquids. *J. Am. Chem. Soc.* **2020**, *142* (8), 3880−3890.
(35) Bumstead, A. M.; Pakamore, I.; Richards, K. D.; Thorne, M. F.; Boyadjieva, S. S.; Castillo-Blas, C.; McHugh, L. N.; Sapnik, A. F.; Keeble, D. S.; Keen, D. A.; Evans, R. C.; Forgan, R. S.; Bennett, T. D. Post-synthetic modification of a metal−organic framework glass. *Chem. Mater.* **2022**, *34* (5), 2187−2196.
(36) Bumstead, A. M.; Castillo-Blas, C.; Pakamore, I.; Thorne, M. F.; Sapnik, A. F.; Chester, A. M.; Robertson, G.; Irving, D. J. M.; Chater, P. A.; Keen, D. A.; Forgan, R. S.; Bennett, T. D. Formation of a meltable purinate metal−organic framework and its glass analogue. *Chem. Commun.* **2023**, *59* (6), 732−735.
(37) Song, J.; Frentzel-Beyme, L.; Pallach, R.; Kolodzeiski, P.; Koutsianos, A.; Xue, W.-L.; Schmid, R.; Henke, S. Modulating Liquid−Liquid Transitions and Glass Formation in Zeolitic Imidazolate Frameworks by Decoration with Electron-Withdrawing Cyano Groups. *J. Am. Chem. Soc.* **2023**, *145* (16), 9273−9284.
(38) Panda, T.; Gupta, K. M.; Jiang, J.; Banerjee, R. Enhancement of CO 2 uptake in iso-reticular Co based zeolitic imidazolate frameworks via metal replacement. *CrystEngComm* **2014**, *16* (22), 4677−4680.
(39) López-Cabrelles, J.; Romero, J.; Abellan, G.; Giménez-Marqués, M.; Palomino, M.; Valencia, S.; Rey, F.; Minguez Espallargas, G. Solvent-free synthesis of ZIFs: A route toward the elusive Fe (II) analogue of ZIF-8. *J. Am. Chem. Soc.* **2019**, *141* (17), 7173−7180.
(40) Lopez-Cabrelles, J.; Miguel-Casan, E.; Esteve-Rochina, M.; Andres-Garcia, E.; Vitorica-Yrezabal, I. J.; Calbo, J.; Minguez Espallargas, G. Multivariate sodalite zeolitic imidazolate frameworks: a direct solvent-free synthesis. *Chem. Sci.* **2022**, *13* (3), 842−847.
(41) León-Alcaide, L.; Christensen, R. S.; Keen, D. A.; Jordá, J. L.; Brotons-Alcázar, I.; Forment-Aliaga, A.; Mínguez Espallargas, G. Meltable, Glass-Forming, Iron Zeolitic Imidazolate Frameworks. *J. Am. Chem. Soc.* **2023**, *145* (20), 11258−11264.
(42) Wu, T.; Bu, X.; Liu, R.; Lin, Z.; Zhang, J.; Feng, P. A New Zeolitic Topology with Sixteen-Membered Ring and Multidimensional Large Pore Channels. *Eur. J. Chem.* **2008**, *14* (26), 7771−7773.
(43) Wu, T.; Bu, X.; Zhang, J.; Feng, P. New zeolitic imidazolate frameworks: from unprecedented assembly of cubic clusters to ordered cooperative organization of complementary ligands. *Chem. Mater.* **2008**, *20* (24), 7377−7382.
(44) Wang, F.; Fu, H.-R.; Kang, Y.; Zhang, J. A new approach towards zeolitic tetrazolate-imidazolate frameworks (ZTIF s) with uncoordinated N-heteroatom sites for high CO 2 uptake. *Chem. Commun.* **2014**, *50* (81), 12065−12068.
(45) Li, H.-Z.; Du, D.-Y.; Sun, Y.; Wang, F.; Zhang, J. Adjustment of the performance and stability of isostructural zeolitic tetrazolate-imidazolate frameworks. *Dalton Trans.* **2020**, *49* (15), 4690−4693.
(46) Li, M.-Y.; Wang, F.; Zhang, J. Water-stable Zeolitic Tetrazolate-Imidazolate Frameworks (ZTIFs) with GIS topology. *Inorg. Chem. Commun.* **2019**, *105*, 59−62.
(47) Zhu, A.-X.; Lin, R.-B.; Qi, X.-L.; Liu, Y.; Lin, Y.-Y.; Zhang, J.-P.; Chen, X.-M. Zeolitic metal azolate frameworks (MAFs) from ZnO/Zn (OH) 2 and monoalkyl-substituted imidazoles and 1, 2, 4-triazoles: Efficient syntheses and properties. *Microporous Mesoporous Mater.* **2012**, *157*, 42−49.
(48) Bergaoui, M.; Khalfaoui, M.; Awadallah-F, A.; Al-Muhtaseb, S. A review of the features and applications of ZIF-8 and its derivatives for separating CO2 and isomers of C3-and C4-hydrocarbons. *Journal of Natural Gas Science and Engineering* **2021**, *96*, 104289.
(49) Zhong, G.; Liu, D.; Zhang, J. The application of ZIF-67 and its derivatives: adsorption, separation, electrochemistry and catalysts. *J. Mater. Chem. A* **2018**, *6* (5), 1887−1899.
(50) Awang Chee, D. N.; Aziz, F.; Mohamed Amin, M. A.; Ismail, A. F. ZIF-8 membrane: the synthesis technique and nanofiltration application. *Emergent Materials* **2022**, *5* (5), 1289−1310.
(51) Chen, B.; Yang, Z.; Zhu, Y.; Xia, Y. Zeolitic imidazolate framework materials: recent progress in synthesis and applications. *J. Mater. Chem. A* **2014**, *2* (40), 16811−16831.
(52) Tranchemontagne, D. J.; Mendoza-Cortés, J. L.; O'keeffe, M.; Yaghi, O. M. Secondary building units, nets and bonding in the chemistry of metal−organic frameworks. *Chem. Soc. Rev.* **2009**, *38* (5), 1257−1283.
(53) Cook, T. R.; Zheng, Y.-R.; Stang, P. J. Metal−organic frameworks and self-assembled supramolecular coordination complexes: comparing and contrasting the design, synthesis, and functionality of metal−organic materials. *Chem. Rev.* **2013**, *113* (1), 734−777.
(54) Smulders, M. M.; Riddell, I. A.; Browne, C.; Nitschke, J. R. Building on architectural principles for three-dimensional metallosupramolecular construction. *Chem. Soc. Rev.* **2013**, *42* (4), 1728−1754.
(55) Ahmad, N.; Younus, H. A.; Chughtai, A. H.; Verpoort, F. Metal−organic molecular cages: applications of biochemical implications. *Chem. Soc. Rev.* **2015**, *44* (1), 9−25.

https://doi.org/10.1021/acs.inorgchem.3c02322
Inorg. Chem. 2023, 62, 20861−20873

(56) Lu, Z.; Knobler, C. B.; Furukawa, H.; Wang, B.; Liu, G.; Yaghi, O. M. Synthesis and structure of chemically stable metal− organic polyhedra. *J. Am. Chem. Soc.* **2009**, *131* (35), 12532−12533.
(57) Vetromile, C. M.; Lozano, A.; Feola, S.; Larsen, R. W. Solution stability of Cu (II) metal−organic polyhedra. *Inorg. Chim. Acta* **2011**, *378* (1), 36−41.
(58) Fujita, M.; Yazaki, J.; Ogura, K. Preparation of a macrocyclic polynuclear complex,[(en) Pd (4, 4'-bpy)] 4 (NO3) 8 (en= ethylenediamine, bpy= bipyridine), which recognizes an organic molecule in aqueous media. *J. Am. Chem. Soc.* **1990**, *112* (14), 5645−5647.
(59) Harris, K.; Fujita, D.; Fujita, M. Giant hollow M n L 2n spherical complexes: structure, functionalisation and applications. *Chem. Commun.* **2013**, *49* (60), 6703−6712.
(60) Masciocchi, N.; Bruni, S.; Cariati, E.; Cariati, F.; Galli, S.; Sironi, A. Extended polymorphism in copper (II) imidazolate polymers: a spectroscopic and XRPD structural study. *Inorg. Chem.* **2001**, *40* (23), 5897−5905.
(61) Hayashi, H.; Côté, A. P.; Furukawa, H.; O'Keeffe, M.; Yaghi, O. M. Zeolite A imidazolate frameworks. *Nat. Mater.* **2007**, *6* (7), No. 501.
(62) Sugiyama, S.; Yamamoto, S.; Matsuoka, O.; Nozoye, H.; Yu, J.; Zhu, G.; Qiu, S.; Terasaki, O. AFM observation of double 4-rings on zeolite LTA crystals surface. *Microporous Mesoporous Mater.* **1999**, *28* (1), 1−7.
(63) Baerlocher, C.; McCusker, L. B.; Olson, D. H. *Atlas of Zeolite Framework Types*; Elsevier, 2007.
(64) Moghadam, P. Z.; Li, A.; Wiggin, S. B.; Tao, A.; Maloney, A. G.; Wood, P. A.; Ward, S. C.; Fairen-Jimenez, D. Development of a Cambridge Structural Database subset: a collection of metal−organic frameworks for past, present, and future. *Chem. Mater.* **2017**, *29* (7), 2618−2625.
(65) Gopalan, A.; Snurr, R. Q. Molecular Siting of C1−C6 n-Alkanes in ZIF-4: A Hybrid Monte Carlo Study. *J. Phys. Chem. C* **2021**, *125* (29), 16256−16267.
(66) Kolokolov, D. I.; Stepanov, A. G.; Jobic, H. Mobility of the 2-methylimidazolate linkers in ZIF-8 probed by 2H NMR: saloon doors for the guests. *J. Phys. Chem. C* **2015**, *119* (49), 27512−27520.
(67) Fairen-Jimenez, D.; Moggach, S.; Wharmby, M.; Wright, P.; Parsons, S.; Duren, T. Opening the gate: framework flexibility in ZIF-8 explored by experiments and simulations. *J. Am. Chem. Soc.* **2011**, *133* (23), 8900−8902.
(68) Hobday, C. L.; Bennett, T. D.; Fairen-Jimenez, D.; Graham, A. J.; Morrison, C. A.; Allan, D. R.; Duren, T.; Moggach, S. A. Tuning the swing effect by chemical functionalization of zeolitic imidazolate frameworks. *J. Am. Chem. Soc.* **2018**, *140* (1), 382−387.
(69) Zhao, P.; Lampronti, G. I.; Lloyd, G. O.; Wharmby, M. T.; Facq, S. b.; Cheetham, A. K.; Redfern, S. A. Phase transitions in zeolitic imidazolate framework 7: the importance of framework flexibility and guest-induced instability. *Chem. Mater.* **2014**, *26* (5), 1767−1769.
(70) Wharmby, M. T.; Henke, S.; Bennett, T. D.; Bajpe, S. R.; Schwedler, I.; Thompson, S. P.; Gozzo, F.; Simoncic, P.; Mellot-Draznieks, C.; Tao, H.; Yue, Y.; Cheetham, A. K. Extreme Flexibility in a Zeolitic Imidazolate Framework: Porous to Dense Phase Transition in Desolvated ZIF-4. *Angew. Chem., Int. Ed.* **2015**, *54* (22), 6447−6451.
(71) Song, J.; Pallach, R.; Frentzel-Beyme, L.; Kolodzeiski, P.; Kieslich, G.; Vervoorts, P.; Hobday, C. L.; Henke, S. Tuning the High-Pressure Phase Behaviour of Highly Compressible Zeolitic Imidazolate Frameworks: From Discontinuous to Continuous Pore Closure by Linker Substitution. *Angew. Chem., Int. Ed.* **2022**, *61* (21), e202117565.
(72) Zhang, H.; Zhao, M.; Lin, Y. Stability of ZIF-8 in water under ambient conditions. *Microporous Mesoporous Mater.* **2019**, *279*, 201−210.
(73) Weng, T.; Schmidt, J. Structure and Thermodynamic Stability of Zeolitic Imidazolate Framework Surfaces. *J. Phys. Chem. C* **2020**, *124* (2), 1458−1468.
(74) Longley, L.; Collins, S. M.; Li, S.; Smales, G. J.; Erucar, I.; Qiao, A.; Hou, J.; Doherty, C. M.; Thornton, A. W.; Hill, A. J.; Yu, X.; Terrill, N. J.; Smith, A. J.; Cohen, S. M.; Midgley, P. A.; Keen, D. A.; Telfer, S. G.; Bennett, T. D. Flux melting of metal−organic frameworks. *Chem. Sci.* **2019**, *10* (12), 3592−3601.
(75) Frentzel-Beyme, L.; Kloß, M.; Kolodzeiski, P.; Pallach, R.; Henke, S. Meltable mixed-linker zeolitic imidazolate frameworks and their microporous glasses: from melting point engineering to selective hydrocarbon sorption. *J. Am. Chem. Soc.* **2019**, *141* (31), 12362−12371.
(76) Zhou, C.; Longley, L.; Krajnc, A.; Smales, G. J.; Qiao, A.; Erucar, I.; Doherty, C. M.; Thornton, A. W.; Hill, A. J.; Ashling, C. W.; Qazvini, O. T.; Lee, S. J.; Chater, P. A.; Terrill, N. J.; Smith, A. J.; Yue, Y.; Mali, G.; Keen, D. A.; Telfer, S. G.; Bennett, T. D. Metal-organic framework glasses with permanent accessible porosity. *Nat. Commun.* **2018**, *9* (1), No. 5042.
(77) Leon-Alcaide, L.; Christensen, R. S.; Keen, D. A.; Jorda, J. L.; Brotons-Alcazar, I.; Forment-Aliaga, A.; Minguez Espallargas, G. Meltable, Glass-Forming, Iron Zeolitic Imidazolate Frameworks. *J. Am. Chem. Soc.* **2023**, *145*, 11258.
(78) Bennett, T. D.; Tan, J.-C.; Yue, Y.; Baxter, E.; Ducati, C.; Terrill, N. J.; Yeung, H. H. -M.; Zhou, Z.; Chen, W.; Henke, S.; Cheetham, A. K.; Greaves, G. N. Hybrid glasses from strong and fragile metal-organic framework liquids. *Nat. Commun.* **2015**, *6* (1), No. 8079.
(79) Fonseca, J.; Gong, T.; Jiao, L.; Jiang, H.-L. Metal−organic frameworks (MOFs) beyond crystallinity: amorphous MOFs, MOF liquids and MOF glasses. *J. Mater. Chem. A* **2021**, *9* (17), 10562−10611.
(80) Bennett, T. D.; Goodwin, A. L.; Dove, M. T.; Keen, D. A.; Tucker, M. G.; Barney, E. R.; Soper, A. K.; Bithell, E. G.; Tan, J.-C.; Cheetham, A. K. Structure and properties of an amorphous metal-organic framework. *Phys. Rev. Lett.* **2010**, *104* (11), 115503.
(81) Bennett, T. D.; Cheetham, A. K. Amorphous metal−organic frameworks. *Acc. Chem. Res.* **2014**, *47* (5), 1555−1562.
(82) Shi, Z.; Arramel, A.; Bennett, T. D.; Yue, Y.; Li, N. The deformation of short-range order leading to rearrangement of topological network structure in zeolitic imidazolate framework glasses. *iScience* **2022**, *25* (6), 104351.
(83) Gaillac, R.; Pullumbi, P.; Beyer, K. A.; Chapman, K. W.; Keen, D. A.; Bennett, T. D.; Coudert, F.-X. Liquid metal−organic frameworks. *Nat. Mater.* **2017**, *16* (11), No. 1149.
(84) Adhikari, P.; Xiong, M.; Li, N.; Zhao, X.; Rulis, P.; Ching, W.-Y. Structure and electronic properties of a continuous random network model of an amorphous zeolitic imidazolate framework (a-ZIF). *J. Phys. Chem. C* **2016**, *120* (28), 15362−15368.
(85) Frentzel-Beyme, L.; Kloß, M.; Pallach, R.; Salamon, S.; Moldenhauer, H.; Landers, J.; Wende, H.; Debus, J.; Henke, S. Porous purple glass−a cobalt imidazolate glass with accessible porosity from a meltable cobalt imidazolate framework. *J. Mater. Chem. A* **2019**, *7* (3), 985−990.
(86) Li, S.; Limbach, R.; Longley, L.; Shirzadi, A. A.; Walmsley, J. C.; Johnstone, D. N.; Midgley, P. A.; Wondraczek, L.; Bennett, T. D. Mechanical properties and processing techniques of bulk metal−organic framework glasses. *J. Am. Chem. Soc.* **2019**, *141* (2), 1027−1034.
(87) Sudharshan Phani, P.; Oliver, W.; Pharr, G. On the measurement of power law creep parameters from instrumented indentation. *Jom* **2017**, *69* (11), 2229−2236.
(88) To, T.; Sørensen, S. S.; Stepniewska, M.; Qiao, A.; Jensen, L. R.; Bauchy, M.; Yue, Y.; Smedskjaer, M. M. Fracture toughness of a metal−organic framework glass. *Nat. Commun.* **2020**, *11* (1), No. 2593.
(89) Sørensen, S. S.; Østergaard, M. B.; Stepniewska, M.; Johra, H.; Yue, Y.; Smedskjaer, M. M. Metal−Organic Framework Glasses Possess Higher Thermal Conductivity than Their Crystalline Counterparts. *ACS Appl. Mater. Interfaces* **2020**, *12* (16), 18893−18903.

https://doi.org/10.1021/acs.inorgchem.3c02322
Inorg. Chem. 2023, 62, 20861−20873